ELSEVIER

Catalysis Today 45 (1998) 353–359

CATALYSIS TODAY

Catalytic functionality of unsupported molybdenum sulfide catalysts prepared with different methods

Y. Iwata[a,*], K. Sato[a], T. Yoneda[a], Y. Miki[b], Y. Sugimoto[b], A. Nishijima[1,b], H. Shimada[b]

[a]*Advanced Catalysts Research Laboratory, Petroleum Energy Center KSP R&D D-12-1237, Sakato 3-2-1, Takatsu, Kanagawa 213, Japan*
[b]*National Institute of Material and Chemical Research, Higashi 1-1, Tsukuba, Ibaraki 305, Japan*

Abstract

The catalytic functionality and structural properties of three kinds of unsupported molybdenum sulfide catalysts were investigated by model test reactions and BET, TEM, XPS and XRD analyses. The results indicated that highly bent multi-layered MoS_2 structures were more catalytically active, while a well crystallized MoS_2 structure was more favorable for direct S-extrusion during the reactions of dibenzothiophene. It was proposed that the curvature of MoS_2 basal planes was catalytically active, though they were less active for hydrodesulfurization than the edge planes.

Keywords: Hydrogenation; Hydrosulfurization; XRD; TEM; MoS_2 structure; Active sites

1. Introduction

Unsupported molybdenum sulfide catalysts have been often used as model catalysts for hydrotreating reactions. In addition, highly dispersed molybdenum sulfide catalysts themselves are a candidate for slurry processes which can accommodate heavy feedstocks with residual matters [1]. From these points of view, there have been a vast amount of experimental data and theoretical studies on molybdenum sulfide catalysts. These studies have indicated that the catalytic activity is closely associated with the edge planes of MoS_2 layers [2–4], in particular with sulfur vacancies formed on the edge sites [5–7]. In spite of the past great efforts, however, some ambiguity still remains on the catalytic functionality of molybdenum sulfide-based catalysts.

The primary purpose of the present study is to discuss the hydrogenation (HY) and hydrodesulfurization (HDS) active sites on unsupported molybdenum sulfide catalysts prepared with different methods. The authors also aim to obtain fundamental information to design high performance powdered catalysts for slurry processes where the catalysts are requested to be effective for the upgrading of heavy feedstocks.

2. Experimental

2.1. Sample preparation

Two kinds of laboratory prepared catalysts (Cat. A and Cat. B) and commercially available MoS_2 powders (Cat. C) were used in the present study. Cat. A was

---

*Corresponding author.

[1] Present address: Kochi Prefectural Industrial Technology Center, Nunoshida 3992-3, Kochi 781-51, Japan.

PII: S0920-5861(98)00262-4

prepared by sulfurization of ammonium heptamolybdate ($(NH_4)_6Mo_7O_{24}\cdot 6H_2O$) in a stream of 10% H_2S/H_2 gas mixture at 450°C for 1 h. Cat. B was a thermally decomposed product of ammonium tetrathiomolybdate ($(NH_4)_2MoS_4$) at 450°C for 1 h in a stream of 10% H_2S/H_2 gas mixture [8].

2.2. Activity measurement

HY and HDS activities of each catalyst were determined using HY of 1-methylnaphthalene (1-MN) and HDS of dibenzothiophene (DBT) as model test reactions. Each reaction feed contained 25 wt% of 1-MN or 5 wt% of DBT with the balance of tetradecane. All the reactions were carried out at 330°C for 1 h in a batch reactor with an inner volume of 35 cm^3. The initial charge to the reactor was 10 cm^3 of feed, 6.0 MPa of H_2 and 0.05–0.20 g of each catalyst. The feed and products were analyzed by GC (HP6890) and GC–MS (HP5970) using a HP Ultra 1 capillary column.

Since the reaction temperature was much lower than for the catalysts preparation, the changes in the catalytic activity and properties during the reactions were assumed to be negligible.

2.3. Catalyst characterization

BET surface area of the catalyst was measured on a Micromeritics ASAP 2010C instrument. Prior to the nitrogen adsorption at 77 K 1–2 g of each catalyst was weighed and degassed at 150°C. X-ray diffraction (XRD) patterns were recorded using a Phillips PW1800 diffractometer (Cu K_α, 40 kV, 40 mA) with a scan speed of 0.02°C/ s and a 2θ range of 5–65°. X-ray photoelectron spectroscopy (XPS) spectra were obtained on a PHI 5500 photoelectron spectrometer using Mg K_α (1253.6 eV). The sample preparation and measurement procedure were carried out carefully so that the catalyst was not exposed to air before analysis. Surface S/Mo ratios were determined using the integrated areas of Mo3d and S2p features. Bulk composition of the catalyst was measured by atomic absorption and emission spectrometry. Transmission electron microscope (TEM) observation was performed with a Hitachi 9000UHR operated at an accelerated voltage of 200 kV. After grinding with a mortar and a pestle, each catalyst sample was ultrasonically dispersed on a copper grid with holey carbon films in monochlorobenzene.

3. Results and discussion

3.1. Catalytic functionality

In the reaction of 1-MN under the present reaction conditions, the major products were 1-methyltetralin (1-MT), 5-methyltetralin (5-MT), methyltetralin isomers, 2,6-methyltetralin and methyldecalins. Since the yields of other compounds were relatively low, the total yield of 1-MT and 5-MT is defined as HY activity here in after. In the reaction of DBT, three kinds of hydrogenated compounds, tetrahydrodibenzothiophene (THDBT), hexahydrodibenzothiophenes (HHDBT), perhydro-dibenzothiophenes (PHDBT) and several desulfurized compounds, biphenyl (BP), cyclohexylbenzenes (CHB), bicyclohexyls (BCH), benzene, cyclohexene, etc. were produced. The total yield of desulfurized compounds is defined as HDS activity.

Fig. 1 shows the changes of HY and HDS activities with the catalyst weight. In both of the 1-MN and DBT reactions, Cat. B exhibits much higher activities than the other two catalysts. The activities of Cat. A and Cat. C are at an almost same level.

Fig. 2 demonstrates the ratio of 5-MT and 1-MT yields in the reaction of 1-MN over various catalysts. The product selectivity is significantly different between conventionally prepared NiMo and molyb-

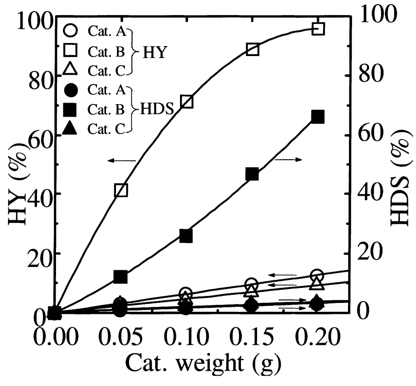

Fig. 1. Catalytic activity of molybdenum sulfide catalysts.

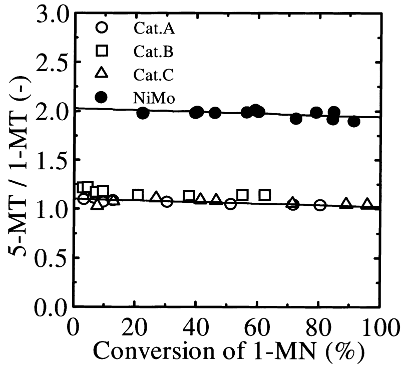

Fig. 2. Catalytic selectivity in HY of 1-MN.

denum sulfide catalysts. The ratio is independent of the catalyst preparation methods among the three unsupported molybdenum sulfide catalysts in spite of the large difference in the catalytic activities. This suggests that the high activity of Cat. B is not likely due to the genesis of highly activities for HY but due to a large number of active sites than Cat. A and Cat. C. The analysis of HY reaction results indicate that the conversion of 1-MN follows a pseudo-first reaction mechanism, $\mathrm{d}[1\text{-MN}]/\mathrm{d}t=-k\mathrm{HY}\ [1\text{-MN}]$, up to the 1-MN conversion of 50%, because the H_2 partial pressure can be assumed to be constant in the above range. Table 1 gives the reaction rate constants over the three catalysts based on the above assumption.

Fig. shows the yields of some typical products in HDS reactions as a function of the total conversion of DBT. The yields of THDBT and HHDBT at the same DBT conversion values decrease in the order of Cat. B>Cat. A>Cat. C as shown in Fig. 3(a) and (b), while the yield of BP is significantly larger over Cat. C than Cat. A and Cat. B (Fig. 3(c)). All the catalysts give similar profiles, as shown in Fig. 3(d), for the total yield of CHB and BCH, which are assumed as final products. These results indicate the differences in reaction pathways among the three catalysts. There have been several studies on the reaction mechanisms of DBT over molybdenum sulfide-based catalysts [9–12]. As a result, it has been concluded that HDS of DBT proceeds through two parallel pathways; one by direct S-extrusion leading to BP, the other by HY of an aromatic ring prior to S-extrusion, as shown in Fig. 4 [9,10]. To clarify the differences in the catalytic features of the three catalysts, we have attempted to determine the rate constants in the network. The employment of the Langmuir–Hinshelwood treatment is essential for the precise analysis of the reaction kinetics, however, the present results do not give enough data for the treatment. As a first approximation, therefore, a pseudo-first order reaction has been assumed for each step of the reaction in the network. The individual rate constants in Table 1 have been determined using the pseudo-first order reaction rate equations in the consecutive reaction system following the manner in [13]. Table 1 summarizes the rate constants thus determined.

The pseudo-first order assumption is oversimplification for HDS of DBT. Nevertheless, the experimental results have been to a large extent simulated using this assumption in the low conversion region. Over Cat. A and Cat. B, the rate constant ratios, k_1/k_{DBT} and k_3/k_{DBT}, which correspond to HY of aromatic rings, are relatively large compared with k_5/k_{DBT} corresponding to direct S-extrusion from the DBT framework. Because of this feature of Cat. A and Cat. B, HY of the aromatic ring preferentially takes place compared with direct S-extrusion in the first step of the reaction and the yields of THDBT and HHDBT are large (Fig. 3(a) and (b)). On the other hand, Cat. C gives larger k_2/k_{DBT} and k_5/k_{DBT} values for direct S-extrusion than the other two catalysts. The relatively large yield of BP over Cat. C is accounted for by the low k_4/k_2 values. Houalla et al. [9] and Edvinsson and Irandoust [11] reported that the main reaction pathway of

Table 1
Rate constants for the 1-MN and DBT reactions over unsupported molybdenum sulfide catalysts

Catalyst	$k_{1\text{-MN}}$	k_{DBT}	$k_1/\mathrm{k}_{\mathrm{DBT}}$	k_2/k_{DBT}	k_3/k_{DBT}	k_4/k_{DBT}	k_5/k_{DBT}	k_4/k_2
Cat. A	35.9	1.74	0.43	0.57	5.24	13.8	0.62	24.3
Cat. B	745	58.5	0.55	0.45	5.60	13.7	0	30.4
Cat. C	26.8	1.55	0.19	0.81	3.92	5.4	1.15	6.7

Rate constants in 10^{-7} mol/(mol Mo) s.

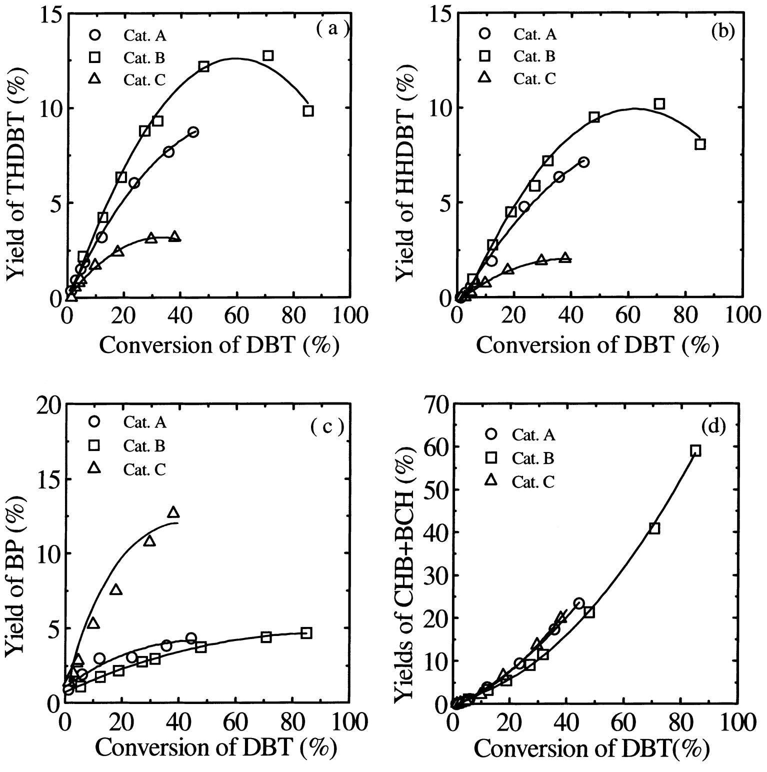

Fig. 3. Product distribution of DBT.

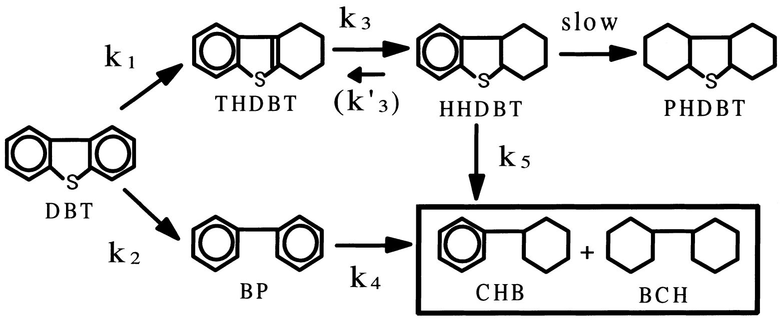

Fig. 4. HDS reaction network of DBT. Note the reverse reaction from HHDBT to THDBT was neglected, because the calculation was made for lower DBT conversion range below 30%. The reaction from HHDBT to PHDBT was neglected since the yield of PHDBT was very low under the present conditions.

DBT was direct S-extrusion via BP over CoMo/Al_2O_3 and NiMo/Al_2O_3 catalysts. Nagai and Kabe [10] claimed that BP was not hydrogenated to CHB and that all the CHB was yielded via THDBT and HHDBT over a Mo/Al_2O_3 catalyst. When the rate constants calculated in the present study are compared with those in these previous studies, the catalytic feature of Cat. C resembles the features reported in the previous studies. On the contrary, HY rate constants over Cat. A and Cat. B are significantly higher than those in previous studies. This is evidenced by much higher yields of hydrogenated intermediate products,

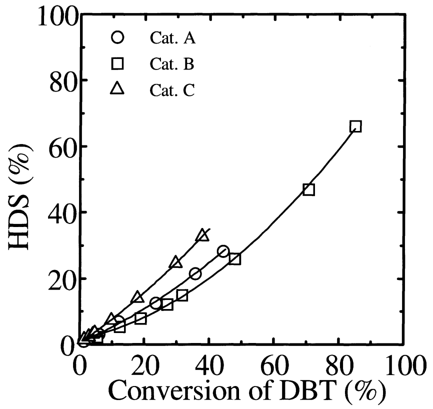

Fig. 5. Relationship between DBT conversion and HDS activity.

such as THDBT and HHDBT. We presume that the catalytic properties of Cat. A and Cat. B prepared in the present study are different from those of the supported catalysts, although the reaction conditions in the present study are not identical to those in the previous studies.

In summary, the kinetic analysis demonstrates the different catalytic features of Cat. A and Cat. B from that of Cat. C. Cat. B gives much larger HY and HDS rate constants than Cat. A and Cat. C. However, the catalytic properties of Cat. B are more-oriented to HY compared with the other two catalysts. This is demonstrated by the lowest sulfur removal over Cat. B at the same DBT conversion levels as shown in Fig. 5. In contrast, the catalytic properties of Cat. C are most favorable for direct S-extrusion, though the rate constant is the lowest.

3.2. *Catalyst characterization*

The surface area values of the three catalysts are not very different as shown in Table 2. The nitrogen adsorption–desorption isotherm profiles for the three catalysts are with type II or III features, indicative of the absence of micro- or meso-porosity. Fig. 6 compares XRD patterns of the three catalysts. The XRD pattern of Cat. A is characteristic of MoO_2, while that of Cat. C is characteristic of MoS_2. The peaks in the pattern of Cat. B are the broadened and overlapped peaks in the pattern of Cat. C. This indicates that Cat. B has a poorly crystallized MoS_2 structure. The crystallite size in the normal direction to the edge plane is estimated at 3 nm using the (0 0 2) reflection and Scherrer's equation. As shown in Table 2, the surface S/Mo ratios of Cat. B and Cat. C are the same as those of the bulk with the stoichiometric MoS_2 structure. In contrast, the surface S/Mo ratio of Cat. A by XPS is much smaller than the stoichiometric value. However, the surface of Cat. A is most likely to be fully sulfided since the information depth by XPS reaches 2–4 nm in the analysis of S_{2p} and Mo_{3d}. It should be noted that the XPS analysis has detected only Mo^{4+} species for molybdenum, which cannot be separated into MoS_2 and MoO_2 species.

Table 2
Characteristics of molybdenum sulfide catalysts

Catalyst	Surface area (m^2/g)	Pore volume (ml/g)	S/Mo (−)	
			Bulk	Suface
Cat. A	5	0.02	0.1	1.1
Cat. B	10	0.05	2.1	2.0
Cat. B	7	0.03	2.0	2.0

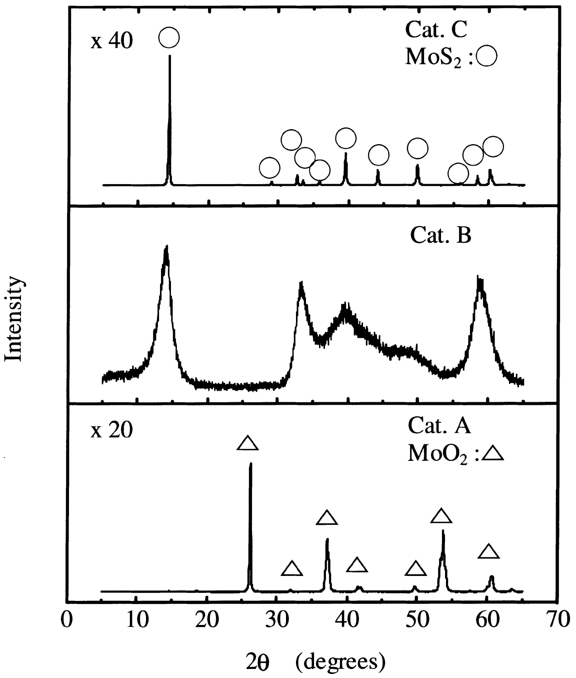

Fig. 6. XRD patterns of Mo sulfide catalysts.

Fig. 7 shows TEM micrographs of the catalysts. The lattice fringes observed in this figure have a

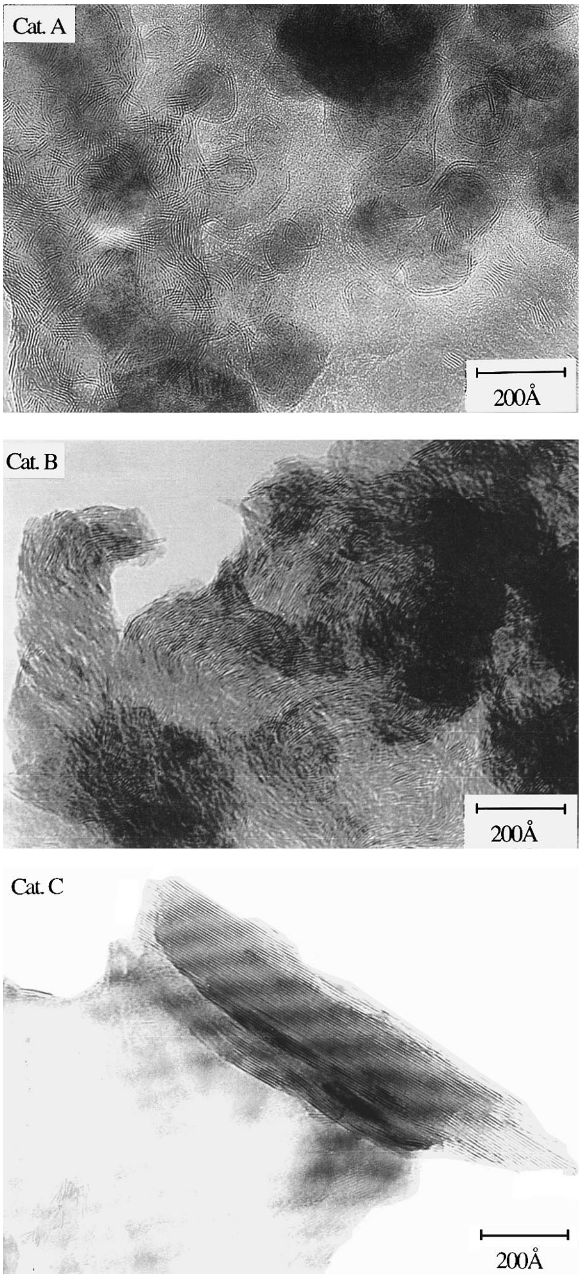

Fig. 7. TEM images of Mo sulfide catalysts.

spacing of about 6 Å that corresponds to the spacing of the (0 0 2) basal planes of MoS_2, 6.15 Å. The TEM image of Cat. A represents a mixture of two different phases. One phase has a bent layered MoS_2 structure with 2–3 layers, the other somewhat an ambiguous structure, which probably corresponds to MoO_2. The image of Cat. B displays a highly bent multi-layered MoS_2 structure in contrast to that of Cat. C with a well crystallized multi-layered MoS_2 structure with no curvature.

Considering both of the XPS and TEM results, Cat. A has a fully sulfided surface with a MoS_2-like structure which surrounds the bulk MoO_2. Cat. B and Cat. C have similar local structures of MoS_2 both at the surface and in the bulk. The structural difference between Cat. B and Cat. C lies in the long-range order of the structure, which gives the distinguished XRD patterns. It should be noted that invisible clusters or an amorphous phase which are not observed by TEM do not exist in the unsupported MoS_2 catalysts [14], since the crystal growth of MoS_2 proceeds homogeneously.

4. Structure–activity relationship

The present results have shown that the poorly MoS_2 crystallized structure of Cat. B with the absence of long-range order provides a larger number of catalytically active sites than the well crystallized structure of Cat. C. The difference in the activity is not accounted for by BET surface area or pore structure. We propose that the catalytically active sites of Cat. B are located not only on the edge planes but also on the curvature of the basal planes of the bent layered MoS_2 structure. It is very likely that some kinds of sulfur vacancies are formed on the curvature.

Some previous studies indicated that the catalytic activity of molybdenum sulfide catalysts were not directly related to BET surface area but dependent on the morphology, in particular on the ratio of basal and edge planes [15]. These discussion are based on the fundamental study by Tanaka and Okuhara [6], which demonstrated that only the edge planes were active. Our above discussion implies that flat basal planes are not catalytically active but bent basal planes possess some catalytic activity. Although the catalytic properties of Cat. A is close to that of Cat. B, the catalytic activity of Cat. A was much lower than Cat. B. This may suggest that HY and HDS functionality is partially affected by the bulk chemical structure.

There have been many studies on the structure-activity relationships of molybdenum sulfide catalysts.

In particular, strong interest has been placed on the different genesis of HY and HDS active sites. In the very early study of unsupported molybdenum sulfide catalysts, Stevens and Edmonds [16] suggested that HY active sites were located at the edge planes of MoS_2 crystallites, while HDS active sites on the basal planes. Massoth and Muralidhar [17] discussed that only the corner sites were active for HDS, while HY were catalyzed on all the edge planes for Mo/Al_2O_3 catalysts. Kasztelan et al. [18] claimed that both reactions were catalyzed on the edge planes based on the geometrical model of unsupported MoS_2. Daage and Chianelli [12] recently discussed that HY of DBT to THDBT occurred exclusively on the top and bottom of edge planes (rim sites) and that direct S-extrusion was catalyzed on all the edge planes. Except the study by Stevens and Edmonds, most of these studies have claimed that all the catalysis takes place on the edge planes which comprise the corner and rim sites. However, some discussions are not consistent with each other as regard to the difference in the HY and HDS functionality of edge planes. The present results suggest the presence of active sites on the curvature of the basal planes in addition to edge planes. Highly bent sites may lead to sulfur vacancies under the reaction conditions which function catalytically active. As shown in the similar $k_{1\text{-MN}}/k_{\text{DBT}}$ ratios given by Cat. B and Cat. C, the catalytically active sites for DBT conversion and HY of 1-MN are more or less common. For direct S-extrusion, however, Cat. C with a well crystallized structure exhibits a comparatively high activity. This implies higher activity of the edge planes than the curvature of the basal planes in terms of direct S-extrusion. Future study is now being carried out on the elucidation of the role of curvature of the basal planes.

5. Conclusion

The present study have correlated the catalytic functionality and structural properties of unsupported molybdenum sulfide catalysts prepared by different methods. Presence of catalytically active sites on the curvature of the basal planes of MoS_2 crystallites has been proposed. However, the intrinsic activity of the active sites on the basal planes is inferior to that of the edge planes active sites in terms of direct S-extrusion.

Acknowledgements

This work has been carried out as a research project of the Petroleum Energy Center with the subsidy of the Ministry of International Trade and Industry.

References

[1] F. Morel, S. Kressmann, V. Harlé, S. Kasztelan, in: Proceedings of the First International Symposium on Hydrotreatment and Hydrocracking of Oil Fractions, 1997, p. 1.

[2] O.P. Bahl, E.L. Evans, J.M. Thomas, Proc. R. Soc. London, Ser. A 386 (1968) 53.

[3] R.J.H. Voorhoeve, J.C.M. Stuiver, J. Catal. 23 (1971) 228.

[4] T. Okuhara, K.I. Tanaka, J. Phys. Chem. 82 (1978) 1953.

[5] R.R. Chianelli, Int. Rev. Phys. Chem. 2 (1982) 127.

[6] K.I. Tanaka, T. Okuhara, Catal. Rev.-Sci. Eng. 15 (1977) 249.

[7] S. Kasztelan, H. Toulhoat, J. Grimblot, J.P. Bonnelle, Appl. Catal. 13 (1984) 127.

[8] A. Muller, E. Diemann, Z. Naturforsch. B 23 (1968) 1607.

[9] M. Houalla, N.K. Nag, A.V. Sapre, D.H. Broderick, B.C. Gates, AIChE J. 24 (1978) 1015.

[10] M. Nagai, T. Kabe, J. Jpn. Pet. Inst. 23 (1980) 82.

[11] R. Edvinsson, A. Irandoust, Ind. Eng. Chem. Res. 32 (1993) 391.

[12] M. Daage, R.R. Chianelli, J. Catal. 149 (1994) 414.

[13] P. Geneste, P. Amblard, M. Bonnet, P. Graffin, J. Catal. 61 (1980) 115.

[14] C. Calais, N. Matsubayashi, C. Geantet, Y. Yoshimura, H. Shimada, A. Nishijima, M. Lacroix, M. Breysse, J. Catal. 174 (1998) 130.

[15] H. Topsøe, B.S. Clausen, F.E. Massoth, Hydrotreating Catalysis, (1996) 157.

[16] G.C. Stevens, T. Edmonds, in: Proceedings of the Second International Conference on The Chemistry and Uses of Molybdenum, Climax Molybdenum Co., 1976, p. 155.

[17] F.E. Massoth, G. Muralidhar, in: Proceedings of the Fourth International Conference on The Chemistry and Uses of Molybdenum, Climax Molybdenum Co., 1982, p. 343.

[18] S. Kasztelan, L. Jalowiecki, A. Wambeke, J. Grimblot, J.P. Bonnelle, Bull. Soc. Chim. Belg. 96 (1987) 1003.